Journal of Physics: Conference Series **1596** (2020) 012018 doi:10.1088/1742-6596/1596/1/012018

Parameter studies on dielectric gratings as electron accelerators

W Kuropka[1,2], R Aßmann[1], U Dorda[1] and F Mayet[1,2]

[1] Deutsches Elektronensynchrotron, Notkestraße 85, 22607 Hamburg, GER
[2] Universität Hamburg, Mittelweg 177, 20146 Hamburg, GER

E-mail: willi.kuropka@desy.de

Abstract. Dielectric laser driven particle acceleration (DLA) is one of the candidates for novel high-gradient technologies to reduce the footprint of large scale particle acceleration facilities. On the other hand these devices can be used to interact with the particle beams of state-of-the-art photon science machines, especially with FELs, to manipulate the longitudinal phase space in a compact and cost effective way. The near-field surface modes of dielectric gratings can be used to interact with particle beams close to the surface. To achieve transversely homogeneous accelerating fields two gratings are opposed. The laser can be coupled from the side into the structure. In this work we present a study on the influence of the geometry parameters of the grating on the acceleration gradient and its transverse uniformity. Based on this study a design for production was chosen, which will be used for experiments at the ARES linac within the SINBAD facility at DESY. This work was carried out within the ACHIP project funded by the Gordon and Betty Moore Foundation (GBMF 4744).

1. SINBAD and ARES

The presented study was conducted within the ACHIP project [1]. The dedicated accelerator research and development site SINBAD at DESY houses the s-band linac ARES, which is in commissioning [2]. This linac will be used to conduct dielectric laser acceleration experiments. Low-emittance, femto-second electron bunches are expected from the machine. These are well suited to be injected into novel particle acceleration schemes. Dielectric laser acceleration structures are a candidate for high acceleration gradients due to the large damage threshold of these materials at optical to near-infrared frequencies.

2. Fused Silica Double Grating

The coupling behavior of a rectangular fused silica double grating is studied with respect to its geometry parameters. A schematic of a single period of the grating and the considered parameters are given in figure 1. The polarization of the incoming laser is also given with the electric field in the direction of the traveling particle beam and incident from one side only. Gratings like that have been used in previous experiments [3].

In this work a longer laser wavelength is chosen compared to previous experiments to increase the electron beam transmission and to increase the minimum necessary electron bunch length to measure the acceleration of an electron beam. The longer wavelength allows for a wider aperture G through which the particle beam will travel in z-direction. The drive laser wavelength used will be 2050 nm from a bandwidth-enhanced Ho:YLF hybrid amplifier [4, 5]. Through parameter

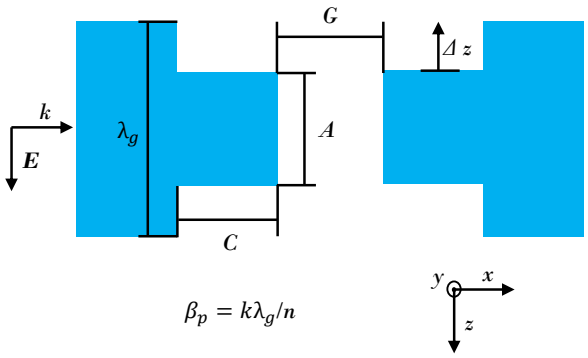

Figure 1. A single period of a dielectric grating. The structure is assumed to be uniform in the y-direction and periodic in z-direction. The schematic illustrates the parameters varied in this study. An electron beam travels in the z-direction through the aperture G. Parameters A and C are the width and height of the grating teeth. λ_g is the period of the grating and Δz the offset of the opposing teeth, if the two opposing gratings are moved against each other in z-direction. The laser field incident in x-direction has an electric field $\boldsymbol{E}$ polarized in z-direction with the wavenumber k. β_p is the relativistic speed of a particle that is matched to the phase velocity of the n-th spatial harmonic in the gap region in accordance with equation 4.

scans using the frequency solver of CST Studio [6] the properties of the electromagnetic fields in the gap of the DLA are studied. The diffraction fields in the double grating gap can be described by a sum of spatial harmonics along the grating surface [7]:

$$E_x = \Re\big[- E_0 \sum_n \frac{k_n}{\Lambda_n} [b_n e^{i\Lambda_n x} - c_n e^{-i\Lambda_n x}] e^{ik_n z}\big] \tag{1}$$

$$E_z = \Re\big[E_0 \sum_n [b_n e^{i\Lambda_n x} + c_n e^{-i\Lambda_n x}] e^{ik_n z}\big] \tag{2}$$

$$B_y = \Re\big[\frac{\omega}{c^2} E_0 \sum_n \frac{1}{\Lambda_n} [b_n e^{i\Lambda_n x} - c_n e^{-i\Lambda_n x}] e^{ik_n z}\big]. \tag{3}$$

E_x and E_z are the non-zero electric field components and B_y is the non-zero magnetic flux density component for the given polarization. The index n is an integer with the wavenumber $k_n = 2\pi n/\lambda_g$ of the spatial harmonics where λ_g is the periodicity of the grating. A harmonic time dependence is assumed with $\omega = 2\pi f$ and the frequency f defined by the laser wavelength $\lambda_l = 2\pi/k$. $\Lambda_n = \sqrt{(\omega/c)^2 - k_n^2}$ gives the transverse dependence of the spatial harmonics in the aperture. In order for the electron beam with the relativistic velocity β_p to be synchronous with the first spatial harmonic the grating period λ_g has to be chosen in accordance with the synchronicity condition that depends on the laser wavelength λ_l:

$$\lambda_g = \beta_p n \lambda_l. \tag{4}$$

The quantity of interest is the ratio of the incoming laser field amplitude E_0 to the amplitude of the n-th spatial harmonic in the middle of the aperture. For $x = 0$ in equation 2 this ratio is equal to the magnitude of the complex number $a_n = b_n + c_n$. The Fourier coefficients a_n can be extracted from the simulated field data. For relativistic particle beams β_p will be close to unity. Figure 2 shows the transverse dependence of the first three spatial harmonics in magnitude and

argument for the single-sided illumination of the grating. The first spatial harmonic that has a speed of light phase velocity is almost uniform over the aperture. This behavior makes a_1 a suitable measure for the investigation. The arguments for very small magnitudes of the second and third spatial harmonic are dominated by a numerical instability and are not meaningful.

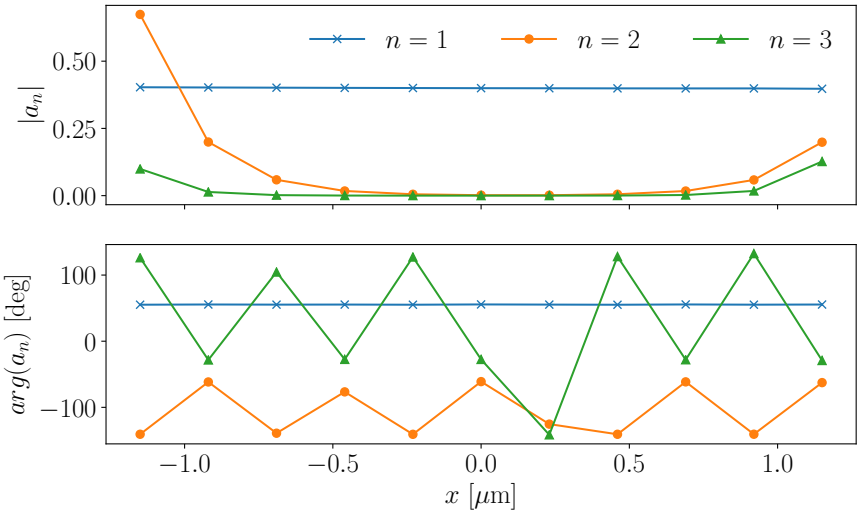

Figure 2. Magnitude and argument of a_n for the first three spatial harmonics using the grating design parameters below in table 1. The first spatial harmonic, which has a speed of light phase velocity in this case, is almost uniform over the DLA aperture. The other two spatial harmonics fall off sharply away from the aperture. The arguments for small magnitudes are meaningless due to numerical instability at near zero input values. The sum over the infinite number of spatial harmonics gives the field in the gap region.

3. Parameter study

The geometric parameters A (width of the grating teeth), C (height of the grating teeth), G (aperture, distance between two opposed gratings), offset of the two opposed gratings Δz and the grating periodicity λ_g are varied to find parameters that are robust against manufacturing tolerances of around 20 nm. The magnitude and the phase of the first spatial harmonic a_1 should not change significantly in this region of interest.

Figure 3 shows the dependence of the Fourier coefficients a_1, a_2 and a_3 of the first three spatial harmonics and a_0 for the fundamental spatial harmonic on the parameters A and C (compare equation 2). The fundamental spatial harmonic has no periodic dependence on z and no transient dependence in x and corresponds to the transmitted laser field through the structure. The higher order spatial harmonics are evanescent surface modes. The first spatial harmonic is used for the relativistic electron beam interaction, due to the matched particle velocity β_p to the speed of light phase velocity. To first order, the influence of the higher order spatial harmonics on a traversing charged particle averages out over a full DLA period.

The dependence of a_1 on the aperture width G was investigated. This is the parameter that sets the transmission for a fixed minimal transverse particle beam size. The results are shown in figure 4. Again a design width is chosen where the magnitude of a_1 is only weakly dependent on G. The amplitude is decreasing exponentially with increasing aperture G as expected from equation 2. Also the etalon behavior is superimposed. The effect is responsible for the plateaus in the plot. Here the gap length G changes the optical path length.

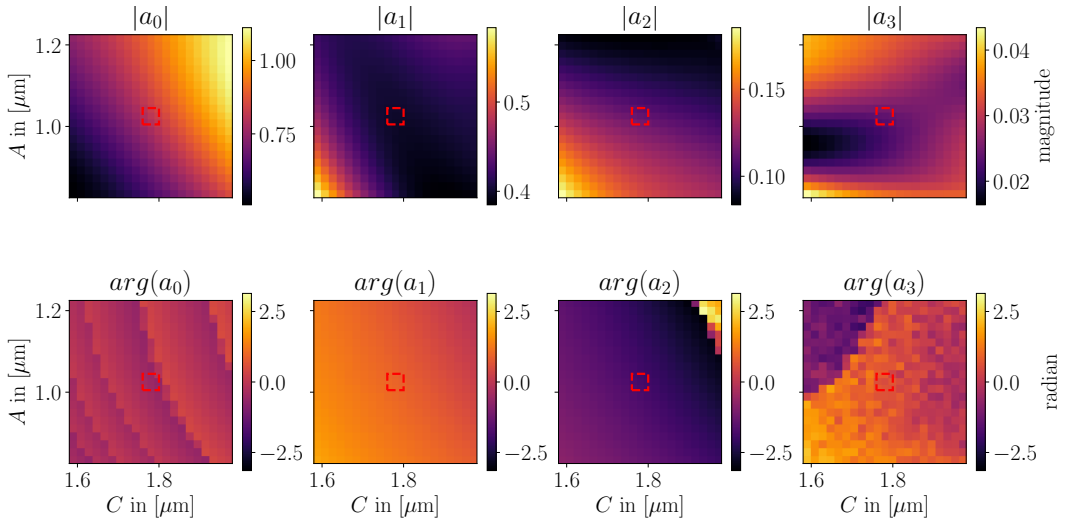

Figure 3. The Fourier coefficients magnitude and argument in radian from the field solver for the fundamental spatial harmonic and the first three higher orders. It can be observed that the evanescent higher order modes have higher magnitudes where the fundamental spatial harmonic has a lower amplitude. The behavior is comparable to that of an etalon for the fundamental. A influences the filling ratio and thus the effective refractive index and C the optical path length. The design parameters are in the center of the plots and the red rectangle gives the 20 nm range around it. The magnitude and the phase of a_1 are flat in that region and do not depend strongly on the parameters.

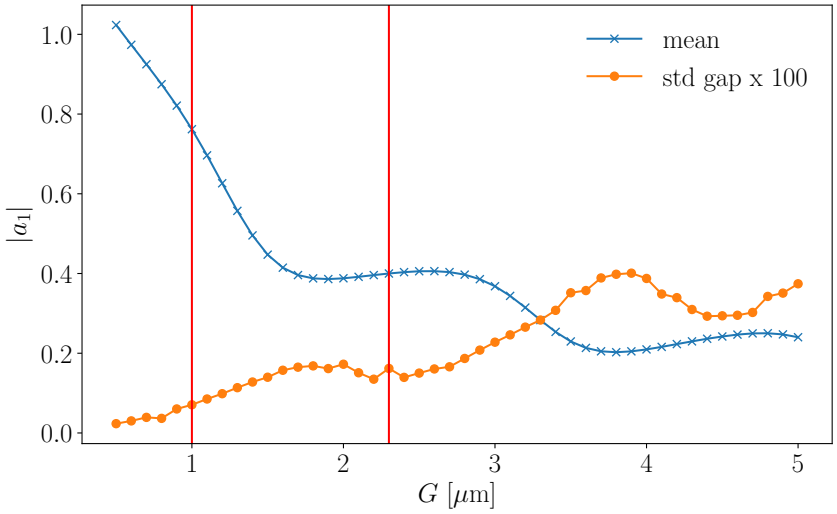

Figure 4. The magnitude of the Fourier coefficients distributed over the aperture of the first spatial harmonic plotted over the DLA aperture G. The blue line is the mean value of the points. As a measure for the uniformity of the first spatial harmonic over the aperture the standard deviation multiplied by 100 is also given by the orange line. The dependence is exponential and an etalon effect is observable by the plateaus. The red vertical lines indicate the two design parameter choices.

The periodicity of the grating influences the phase velocity of the spatial harmonics. We design the DLA to match the first spatial harmonic to a relativistic particle beam. Figure 5 shows the dependence of the magnitude of a_1 on the periodicity. The coupling behavior of a_1 for β_p close to unity shows no strong dependence.

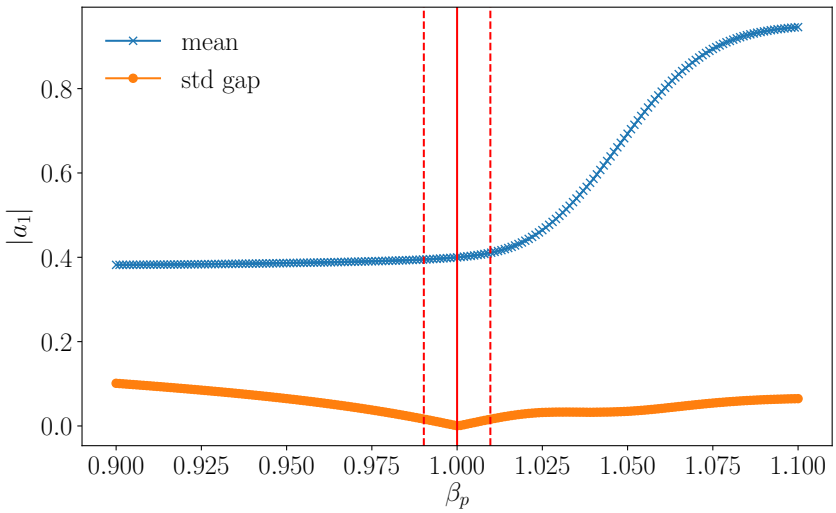

Figure 5. The magnitude of the Fourier coefficients distributed over the aperture of the first spatial harmonic plotted over β_p which is dependent on the grating period λ_g as shown in figure 1. The blue line shows the mean value over the aperture and the orange line shows the standard deviation as a measure of uniformity. The red vertical line indicates the design value of $\beta_p = 1$, which corresponds to $\lambda_g = 2050\,\text{nm}$, the dependence is weak. The broken lines indicate the 20 nm range.

The parameter with the highest manufacturing uncertainty is the offset Δz between the two gratings. The two single gratings are manufactured independently and are later bonded eutectically. This process has a manufacturing tolerance in the order of the grating period λ_g. The dependence of the coupling to the first spatial harmonic is plotted in figure 6. The actual Δz in a manufactured grating will be random.

The total length $L = 1000\,\mu\text{m}$ of the grating DLA was chosen to maximize the absolute energy change with the laser parameters and the electron beam parameters available at SINBAD in accordance with the material dependent laser induced damage threshold and manufacturing capabilities. Table 1 shows the final design parameters.

Table 1. Design parameters for the DLA

Parameter	Value
A	1.025 µm
C	1.78 µm
G	1.0 µm or 2.3 µm
P	2.05 µm
L	1000 µm

Assuming the worst case coupling from figure 6 acceleration gradients of approximately

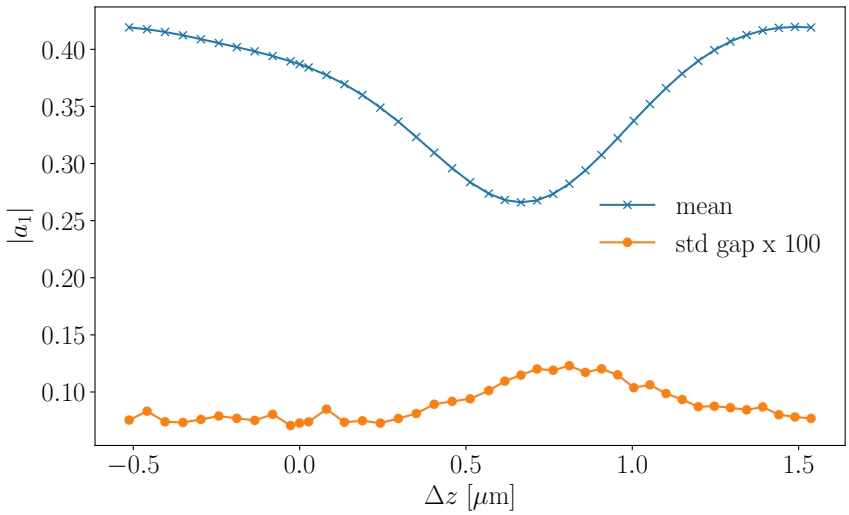

Figure 6. The magnitude of the Fourier coefficients distributed over the aperture of the first spatial harmonic plotted over the offset between the gratings Δz. The blue line is the mean of the points over the aperture and the orange line is the standard deviation as a measure of uniformity. The actual value of Δz in a fabricated device will be random due to the large manufacturing tolerance for this parameter. In the worst case the coupling is $|a_1| = 0.27$.

1 GV/m are predicted and a maximum absolute energy change of 300 keV is expected. By applying the pulse front tilt technique as employed in [8] the absolute energy change can be increased to around 1 MeV. The short electron bunches predicted to be available at ARES would enable an injection into one laser period, thus enabling directly measurable particle beam energy gain.

4. Conclusion

A robust design against manufacturing tolerances for a fused silica grating-type DLA has been devised by simulation. Due to the longer drive laser wavelength the electron transmission is expected to be around 44 % of the total charge with the expected ARES working points from simulations and the wider aperture $G = 2.3\,\mu$m. This is a predicted increase of more than an order of magnitude compared to [3, 8] while maintaining giga-volt per meter acceleration gradients and possibly net energy gain of relativistic electron bunches under the considered manufacturing uncertainties of grating tooth errors, error in periodicity, aperture and alignment of the two opposed gratings.

The experimental area at ARES is under construction and the first baseline experiment is foreseen to be conducted in fall 2020. The arrival time jitter at the interaction point is predicted to be larger than the DLA period so for each electron bunch the laser to electron bunch phase is randomly distributed. If the electron bunch length is shorter than the DLA period the mean bunch length of a set of bunches can be estimated by recording each spectrum and comparison with calculations opening up particle beam diagnostic applications for DLA. The arrival time jitter can be reduced by applying a technique from seeded free electron laser operation. A longer electron bunch can be sinusoidally energy modulated in longitudinal direction via interaction with a laser beam in an undulator, which is called a laser modulator. The energy modulation can be turned into a longitudinal charge density modulation using a dispersive particle beam line element like a chicane. After that the DLA interaction is placed. If the laser modulator and the DLA are driven by the same laser the arrival time jitter at DLA is reduced to the phase

stability between the two laser beam line arms leading to the modulator and the DLA [9]. The implementation of this second stage DLA experiment at the ARES linac planned for the end of the year.

Acknowledgments

This work was conducted within the ACHIP collaboration funded by Gordon and Betty Moore Foundation (GBMF4744). The authors want to thank all ACHIP collaborators and DESY colleagues. The DLA structures have been produced by Y. Miao working at the Solgaard group of Stanford University. Another design for silicon double pillar structures was devised by the same methods and produced by J. Illmer at the Laser group of Friedrich-Alexander-Universität Erlangen. The mounting system for the DLA in the experimental area was produced by the Paul-Scherrer-Institut in collaboration with R. Ischebeck and B. Hermann.

References

[1] Accelerator on a chip international program URL `https://achip.stanford.edu/ (18.12.2019 15:50)`
[2] Dorda U *et al.* 2017 The Dedicated Accelerator R&D Facility Sinbad at DESY (*International Particle Accelerator Conference* no 8) (Geneva, Switzerland: JACoW) ISBN 978-3-95450-182-3 URL `http://jacow.org/ipac2017/papers/mopva012.pdf`
[3] Peralta E A, Soong K, England R J, Colby E R, Wu Z, Montazeri B, McGuinness C, McNeur J, Leedle K J, Walz D, Sozer E B, Cowan B, Schwartz B, Travish G and Byer R L 2013 *Nature* **503** 91–94
[4] Murari K, Cankaya H, Kroetz P, Cirmi G, Li P, Ruehl A, Hartl I and Kärtner F X 2016 *Opt. Lett.* **41** 1114–1117 URL `http://ol.osa.org/abstract.cfm?URI=ol-41-6-1114`
[5] Murari K, Stein G J, Cankaya H, Debord B, Gérôme F, Cirmi G, Mücke O D, Li P, Ruehl A, Hartl I, Hong K H, Benabid F and Kärtner F X 2016 *Optica* **3** 816–822 URL `http://www.osapublishing.org/optica/abstract.cfm?URI=optica-3-8-816`
[6] CST URL `https://www.cst.com/ (18.12.2019 15:50)`
[7] Pilozzi L, D'Andrea A and Del Sole R 1996 *Phys. Rev. B* **54**(15) 10751–10762 URL `https://link.aps.org/doi/10.1103/PhysRevB.54.10751`
[8] Cesar D, Maxson J, Shen X, Wootton K P, Tan S, England R J and Musumeci P 2018 *Opt. Express* **26** 29216–29224 URL `http://www.opticsexpress.org/abstract.cfm?URI=oe-26-22-29216`
[9] Mayet F, Aßmann R, Brinkmann R, Dorda U, Kuropka W, Lechner C, Marchetti B, Zhu J and Boedewadt J 2017 A Concept for Phase-Synchronous Acceleration of Microbunch Trains in DLA Structures at SINBAD *JACoW* 8th International Particle Accelerator Conference, Copenhagen (Denmark), 14 May 2017 - 19 May 2017 (Geneva: JACoW) pp 3260–3263 ISBN 978-3-95450-182-3 URL `http://bib-pubdb1.desy.de/record/392191`